DOI: 10.1021/ic9025238

Inorganic Chemistry
Article

# Electrooxidation of $[(\eta^5\text{-}C_5H_5)Fe(CO)_2]_2$ As a Probe of the Nucleophilic Properties of Ionic Liquid Anions

**Angel A. J. Torriero,[†,‡] Muhammad J. A. Shiddiky,[†] John P. Bullock,[§] John F. Boas,[∥] Douglas R. MacFarlane,[†] and Alan M. Bond*[,†,‡]**

[†]*School of Chemistry,* [‡]*ARC Special Research Centre for Green Chemistry, and* [∥]*School of Physics, Monash University, Clayton, Victoria 3800, Australia, and* [§]*The Division of Natural Science and Mathematics, Bennington College, Bennington, Vermont 05201*

Received December 18, 2009

The oxidative electrochemistry of $[CpFe(CO)_2]_2$, **1** ($Cp = [\eta^5\text{-}C_5H_5]^-$), was examined in detail in ionic liquids (ILs) composed of ions of widely varying Lewis acid−base properties. Cyclic voltammetric responses were strongly dependent on the nucleophilic properties of the IL anion, but all observations are consistent with the initial formation of $\mathbf{1}^+$ followed by attack from the IL anion. In $[NTf_2]^-$-based ILs ($[NTf_2]^-$ = bis(trifluoromethylsulfonyl)amide), the process shows nearly ideal chemical reversibility as the reaction between $\mathbf{1}^+$ and $[NTf_2]^-$ is very slow. This is highly significant, as $\mathbf{1}^+$ is known to be highly susceptible to nucleophilic attack and its stability indicates a remarkable lack of coordinating ability of these ILs. In 1-methyl-3-butylimidazolium hexafluorophosphate, [bmim][$PF_6$], the oxidation of **1** is still largely reversible, but there is more pronounced evidence of $[PF_6]^-$ coordination. In contrast, **1** exhibits an irreversible two-electron oxidation process in a dicyanamide-based IL. This overall oxidation process is thought to proceed via an ECE mechanism, details of which are presented. Rate constants were estimated by fitting the experimental data to digital simulations of the proposed mechanism. The use of $[NTf_2]^-$-based ILs as a supporting electrolyte in $CH_2Cl_2$ was examined by using this solvent/electrolyte as a medium in which to perform bulk electrolyses of **1** and **1***, the permethylated analogue $[Cp^*Fe(CO)_2]_2$ ($Cp^* = [\eta^5\text{-}C_5(CH_3)_5]^-$). These cleanly yielded the corresponding binuclear radical-cation species, $\mathbf{1}^+$ and $\mathbf{1}^{*+}$, which were subsequently characterized by electron paramagnetic resonance (EPR) spectroscopy. In addition to the above oxidation studies, the reduction of **1** was studied in each of the ILs; differences in cathodic peak potentials are attributed, in part, to ion-pairing effects. This study illustrates the wide range of electrochemical environments available with ILs and demonstrates their utility for the investigation of the redox properties of metal carbonyls and other organometallic compounds.

## 1. Introduction

Interest in ionic liquids (ILs) continues to increase at a rapid rate because of their diverse physical and chemical properties.[1,2] They have been widely employed as media for electrochemical studies, in which they can simultaneously serve as both the solvent and the electrolyte.[3] Significantly, they have a number of properties that can substantially modify the electrochemical response of a given redox couple from that obtained when using molecular solvents with added supporting electrolyte. The high viscosities of many IL media, for example, can dramatically lower the diffusion coefficients of electroactive species which, in turn, substantially alters mass transport. More subtly, the kinetics of an electron transfer process can be influenced by the structure of the IL since the energetics of the electrode process are sensitive to solvation effects of the relevant species. In molecular solvents, these solvation effects can involve dipole−dipole interactions between solvent and solute, as well as other intermolecular forces such as hydrogen bonding, $\pi$-interactions, or London dispersion forces. ILs are more complicated than molecular solvents, however, since both the cations and the anions will have their own distinct interactions with the analyte.[4,5]

As with traditional solvent/electrolyte media,[6] ILs can also play a direct role in chemical reactions coupled to electron transfer processes. Accordingly, there is an obvious need to characterize the nucleo- or electrophilicities of ILs. While studies on the role of molecular solvents and/or electrolytes in

*To whom correspondence should be addressed. E-mail: alan.bond@sci.monash.edu.au. Fax: +61 3 9905 4597. Phone: +61 3 9905 1177.

(1) Hapiot, P.; Lagrost, C. *Chem. Rev.* **2008**, *108*, 2238.
(2) Welton, T. *Chem. Rev.* **1999**, *99*, 2071.
(3) Torriero, A. A. J.; Bond, A. M. Critical Evaluation of Electrochemistry in Ionic Liquids. In *Electroanalytical Chemistry Research Trends*; Hayashi, K., Ed.; Nova Science Publishers, Inc.: New York, 2009; Chapter 1.
(4) Aki, S. N. V. K.; Brennecke, J. F.; Samanta, A. *Chem. Commun.* **2001**, 413.
(5) Muldoon, M. J.; Gordon, C. M.; Dunkin, I. R. *J. Chem. Soc., Perkin Trans. 2* **2001**, 413.
(6) Barriere, F.; Geiger, W. E. *J. Am. Chem. Soc.* **2006**, *128*, 3980.


Published on Web 02/01/2010

organometallic redox systems have been widely studied for many years,[7−9] it is perhaps surprising that analogous studies in IL media have yet to be reported. Similarly, despite the fact that there have been some detailed studies examining how the nucleophilicity of solutes can be influenced in IL media,[7,10−13] little attention has been paid to the reactivity of the IL component ions themselves.[14−17]

To probe the reactivity of IL anions and cations toward electrogenerated species, we investigated the redox chemistry of cyclopentadienyliron(I) dicarbonyl dimer, $[CpFe(CO)_2]_2$, **1**, in a range of IL media. This particular system was selected because its electron transfer and coupled chemical reaction pathways have been well-characterized in conventional media and found to vary substantially with the nature of the molecular solvent.[18−21] For example, initial reports of the electrooxidation of **1** in coordinating solvents, such as acetonitrile ($Bu_4NPF_6$),[18] indicated a net two-electron process yielding the corresponding monomeric solvent adduct cation, **2** (eq 1).

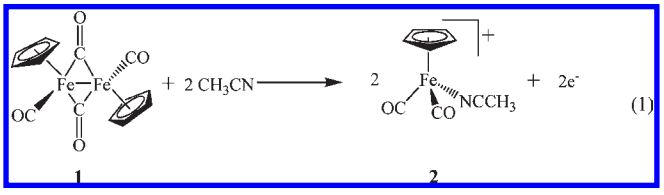


This overall two-electron oxidation proceeds via an ECE mechanism[21] in which the initially formed binuclear one-electron oxidation product, $\mathbf{1}^+$, undergoes rapid reaction with the solvent. In contrast, in less coordinating media such as $CH_2Cl_2$ ($Bu_4NPF_6$), a chemically reversible one-electron processes is observed[19] in which $\mathbf{1}^+$ is stable enough to be generated by bulk electrolysis (BE) at room temperature.

The susceptibility of $\mathbf{1}^+$ to nucleophilic attack by the solvent and/or supporting electrolyte[21,22] makes the electrochemical oxidation of **1** an excellent system with which to examine the chemical reactivity of IL media. This work describes the oxidative and reductive electrochemistry of **1** in four different ILs; structures of the specific anions and cations employed in the ILs are illustrated in Scheme 1. The anions employed in these studies, hexafluorophosphate, $[PF_6]^-$, bis(trifluoromethylsulfonyl)amide, $[NTf_2]^-$, and dicyanamide, $[N(CN_2)]^-$, cover a wide range of Lewis basicities and, as will be described, exhibit markedly different reactivity toward electron-deficient species. The oxidative electrochemical behavior can be explained by the initial generation of $\mathbf{1}^+$ and its subsequent reactivity toward the IL anion. To a lesser extent, the cations employed, 1-methyl-3-butylimidazolium, $[bmim]^+$, 1-methyl-3-ethylimidazolium, $[emim]^+$, L-methyl-1-butylpyrrolidinium, $[bmpyr]^+$, also affect the reductive electrochemistry of **1**. In addition, the oxidation of **1** and its pentamethylcylopentadienyl analogue, $[Cp^*Fe(CO)_2]_2$, **1*** ($Cp^* = [\eta^5\text{-}C_5(CH_3)_5]^-$), were also examined in $CH_2Cl_2$ with IL added to serve as supporting electrolyte. The present study therefore demonstrates the substantial range of electrochemical environments available with ILs, and exemplifies the importance of the reactivities of both the anions and the cations on electrochemical studies performed in IL media.

**Scheme 1.** Structures of Anions and Cations Employed in the Present Study[a]

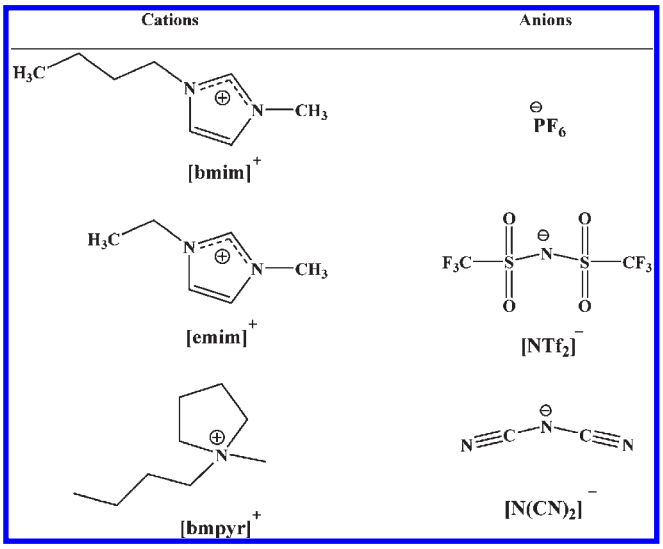


[a] The specific ILs employed were $[bmim][PF_6]$, $[emim][NTf_2]$, $[bmpyr][NTf_2]$, and $[bmpyr][N(CN)_2]$.

## 2. Experimental Section

**Reagents.** High purity grade (> 99.9%) 1-methyl-3-butylimidazolium hexafluorophosphate, $[bmim][PF_6]$, 1-methyl-3-ethylimidazolium bis(trifluoromethylsulfonyl)amide, $[emim][NTf_2]$, 1-methyl-1-butylpyrrolidinium bis(trifluoromethylsulfonyl)amide, $[bmpyr][NTf_2]$, and 1-methyl-1-butylpyrrolidinium dicyanamide, $[bmpyr][N(CN)_2]$, were purchased from Merck. Reagent-grade dichloromethane, $CH_2Cl_2$ (Merck), was distilled from appropriate drying agents and stored over $CaH_2$ prior to use. Acetonitrile (Merck), cobaltocenium hexafluorophosphate, $CcPF_6$ (Strem), cyclopentadienyliron(I) dicarbonyl dimer, **1** (Strem), and pentamethylcyclopentadienyliron(I) dicarbonyl dimer, **1***(Strem), were used as received. Tetrabutylammonium hexafluorophosphate, $Bu_4NPF_6$ (GFS), was recrystallized twice from ethanol before use.

**Apparatus and Procedures.** Experimental procedures were performed in a glovebox under nitrogen. Glassware used for electrochemical experiments was rinsed with nanopure water prior to drying at 120 °C for at least 12 h; hot glassware was cooled under vacuum immediately prior to use.

All potentials are reported relative to the reduction of $CcPF_6$, which was employed as an internal standard in this study. The $CcPF_6$ was added at the end of each set of experiments to ensure no interference with the complex of interest. Voltammetric

(7) Williams, D. B.; Stoll, M. E.; Scott, B. L.; Costa, D. A.; Oldham, W. J., Jr. *Chem. Commun.* **2005**, 1438.
(8) Magna, L.; Chauvin, Y.; Niccolai, G. P.; Basset, J.-M. *Organometallics* **2003**, *22*, 4418.
(9) Earle, M. J.; Hakala, U.; McAuley, B. J.; Nieuwenhuyzen, M.; Ramani, A.; Seddon, K. R. *Chem. Commun.* **2004**, 1368–1369.
(10) Crowhurst, L.; Lancaster, N. L.; Perez Arlandis, J. M.; Welton, T. *J. Am. Chem. Soc.* **2004**, *126*, 11549.
(11) Lancaster, N. L.; Welton, T.; Young, G. B. *J. Chem. Soc., Perkin Trans. 2* **2001**, 2267.
(12) Lancaster, N. L.; Salter, P. A.; Welton, T.; Young, G. B. *J. Org. Chem.* **2002**, *67*, 8855.
(13) Bini, R.; Chiappe, C.; Marmugi, E.; Pieraccini, D. *Chem. Commun.* **2006**, 897.
(14) Raabe, I.; Wagner, K.; Guttsche, K.; Wang, M.; Grätzel, M.; Santiso-Quiñones, G.; Krossing, I. *Chem.—Eur. J.* **2009**, *15*, 1966.
(15) Babai, A.; Mudring, A. V. *Inorg. Chem.* **2006**, *45*, 3249.
(16) Babai, A.; Mudring, A. V. *Dalton Trans.* **2006**, 1828.
(17) Babai, A.; Mudring, A. V. *Z. Anorg. Allg. Chem.* **2008**, *634*, 938.
(18) Ferguson, J. A.; Meyer, T. J. *Inorg. Chem.* **1971**, *10*, 1025.
(19) Legzdins, P.; Wassink, B. *Organometallics* **1984**, *3*, 1811.
(20) Ferguson, J. A.; Meyer, T. J. *Inorg. Chem.* **1972**, *11*, 631.
(21) Bullock, J. P.; Palazotto, M. C.; Mann, K. R. *Inorg. Chem.* **1991**, *30*, 1284.
(22) Hill, M. G.; Lamanna, W. M.; Mann, K. R. *Inorg. Chem.* **1991**, *30*, 4687.

**Table 1.** Cyclic Voltammetric Data Obtained for Oxidation of 7 mM **1** in ILs

| IL | $v$ (V/s) | $10^6\ I_p^{ox}$ (A) | $\Delta E_p$ (mV) | $E_m$ (V)[a] | $E_p - E_{p/2}$ (mV) | $E_p^{red}$ (V)[b] | $I_p^{red}/I_p^{ox}$ | $10^7\ D$ (cm$^2$ s$^{-1}$)[c] | $k_1$ (s$^{-1}$)[d] |
|---|---|---|---|---|---|---|---|---|---|
| [bmpyr][$NTf_2$] | 0.10 | 1.35 | 65 | 1.53 | 61 | −0.67 | 0.81 | 1.05 | 0.58 |
| | 0.20 | 1.90 | 72 | | | | 0.81 | | |
| | 0.40 | 2.60 | 80 | | | | 0.87 | | |
| | 0.70 | 3.50 | 76 | | | | 0.87 | | |
| | 1.00 | 4.03 | 85 | | | | 0.90 | | |
| [emim][$NTf_2$] | 0.10 | 1.81 | 65 | 1.54 | 59 | −0.63 | 0.83 | 1.45 | 0.48 |
| | 0.20 | 2.30 | 70 | | | | 0.80 | | |
| | 0.40 | 3.16 | 75 | | | | 0.86 | | |
| | 0.70 | 4.11 | 75 | | | | 0.86 | | |
| | 1.00 | 5.19 | 75 | | | | 0.87 | | |
| [bmim][$PF_6$] | 0.10 | 0.72 | 69 | 1.54 | 62 | −0.62 | 0.70 | 0.25 | 1.50 |
| | 0.20 | 1.00 | 72 | | | | 0.72 | | |
| | 0.40 | 1.40 | 78 | | | | 0.77 | | |
| | 0.70 | 1.80 | 81 | | | | 0.79 | | |
| | 1.00 | 2.15 | 84 | | | | 0.79 | | |
| [bmpyr][$N(CN)_2$] | 0.10 | 4.02 | | 1.39 | 70 | −0.68 | | 3.60 | 450 |
| | 0.20 | 5.48 | | | | | | | |
| | 0.40 | 7.38 | | | | | | | |
| | 0.70 | 9.39 | | | | | | | |
| | 1.00 | 11.2 | | | | | | | |

[a] Midpoint potential ($E_m$) for oxidation of **1** vs $Cc^{+/0}$, where $E_m$ was calculated from the average of the oxidation ($E_p^{ox}$) and reduction ($E_p^{red}$) peak potentials and is approximately equal to the reversible formal potential ($E_f°$). [b] Peak potentials for the reduction of **1** to **4** (eq 3). [c] $D$ = Diffusion coefficient for **1** calculated from chronocoulometry and cyclic voltammetry. [d] Pseudo-first order kinetic rate constant obtained by the best fit of experimental and simulated voltammograms.

experiments with stationary working electrodes were performed with a BAS 100B/W electrochemical workstation (Bioanalytical System, West Lafayette, IN). Uncompensated resistance was measured in a potential region where no Faradaic reaction occurs,[23] using the RC time constant method available with the instrument. A standard three electrode arrangement was used in voltammetric studies. The working electrode for cyclic voltammetry was a 1.0 mm diameter glassy carbon (GC, effective area = 0.7 mm$^2$) disk (Cypress Systems, Inc., Lawrence, KS). Rotating disk experiments employed a GC working electrode (3.0 mm diameter, 7.1 mm$^2$ effective area), and were performed with a BAS RDE-2 accessory. Working electrodes were polished with 0.3 $\mu$m alumina (Buehler, Lake Bluff, IL) prior to each experiment. The Randles-Sevcik equation was used to calculate effective areas of working electrodes employed in CV studies by using peak currents from the cyclic voltammetric oxidation of ferrocene (diffusion coefficient of $2.3 \times 10^{-5}$ cm$^2$ s$^{-1}$) in acetonitrile (0.1 M $Bu_4NPF_6$). The area of the rotating disk electrode was similarly determined using the Levich equation.[24] A platinum wire served as the counter electrode in all experiments. For experiments conducted in neat IL media, a silver wire quasi-reference (QRE) was separated from the test solution by a glass frit. Experiments performed in dichloromethane with the IL as the supporting electrolyte employed an Ag/AgCl ($CH_2Cl_2$, 0.50 M [bmpyr][$NTf_2$]) single junction quasi-reference electrode.

Bulk electrolyses were performed using a glassy carbon tube working electrode and a platinum gauze auxiliary electrode separated from the analyte solution by a fine porosity glass frit. All voltammetric experiments were carried out at ambient temperature (21 ± 1 °C).

Unless otherwise stated, the concentration of water in IL media was 80 ± 10 ppm, as determined with a Model 756 Karl Fischer Coulometer (Metrohm) using hydranal Coulomat AG as the titrant. Viscosity was determined in a glovebox from triplicate measurements carried out using a calibrated AMVn viscometer.

X-band (ca. 9.3 GHz) electron paramagnetic resonance (EPR) spectra were obtained with the standard $TE_{012}$ rectangular cavity using a Bruker ESP380E CW/FT spectrometer. Sample temperatures between 110 and 175 K were achieved using a Bruker VT4111 temperature controller; spectra measured at 77 K were obtained using a quartz finger dewar. Microwave frequencies were measured with an EIP Microwave 548A frequency counter; g-values were determined with reference to the $F^+$ line in CaO (g-value 2.0001 ± 0.0001).[25] EPR simulations were performed using the X-EPR-X-SOPHE-XEPRVIEW software suite.[26]

## 3. Results and Discussion

ILs may conveniently be classified according to the Lewis acidity or basicity of their component cations and anions.[27] The basicities of the three anions employed in this work follow the order $[NTf_2]^- < [PF_6]^- \ll [N(CN)_2]^-$; the first two are typically considered neutral while the last, dicyanamide, is distinctly basic and is a well-known ligand. A summary of the electrochemical data for oxidation and reduction of **1** in each of the ILs is presented in Table 1.

**3.1. Electrochemistry of 1 in the Basic [bmpyr][$N(CN)_2$] IL.** Dicyanamide-based ILs are potentially important in electrochemical applications because of their generally low viscocities and high conductivities (those of [bmpyr][$N(CN)_2$] are 41 cP and 10.2 mS cm$^{-1}$ at 20 °C).[28] Dicyanamide can form coordinate bonds to transition metal complexes via the terminal nitrile functionalities, sometimes in a bridging fashion, although coordination via the central nitrogen also has been observed.[29] This anion, therefore, has the ability to provide ILs with coordination properties similar to solvents such as acetonitrile.

Figure 1A shows the cyclic voltammogram of **1** in [bmpyr][$N(CN)_2$] obtained at a scan rate of 0.1 V s$^{-1}$. Two bulk processes are observed: an irreversible oxidation at 1.39 V (indicated as peak Ia) and an irreversible reduction at −0.68 V versus $Cc^{+/0}$ (peak IIc). Since the

(23) He, P.; Faulkner, L. R. *Anal. Chem.* **1986**, *58*, 517.
(24) Nuzzo, R. G.; Allara, D. L. *J. Am. Chem. Soc.* **1983**, *105*, 4481.
(25) Wertz, J. E.; Orton, J. W.; Auzins, P. *Faraday Discuss.* **1961**, *31*, 140.
(26) Hanson, G. R.; Gates, K. E.; Noble, C. J.; Griffin, M.; Mitchell, A.; Benson, S. *J. Inorg. Biochem.* **2004**, *98*, 903.
(27) MacFarlane, D. R.; Pringle, J. M.; Johansson, K. M.; Forsyth, S. A.; Forsyth, M. *Chem. Commun.* **2006**, 1905.
(28) MacFarlane, D. R.; Forsyth, S. A.; Golding, J.; Deacon, G. B. *Green Chem.* **2002**, *4*, 444.
(29) Albores, P.; Rentschler, E. *Inorg. Chem.* **2008**, *47*, 7960.

cyclic voltammetry resembles that previously reported in $CH_3CN$,[21] by analogy we assign processes Ia and IIc to the oxidative and reductive cleavage of the formal iron−iron bond, respectively. Specifically, we propose that the final oxidation product is the dicyanamide-coordinated monomer, $CpFe(CO)_2(N(CN)_2)$, **3**, and the reduction product is the monomeric anion, $[CpFe(CO)_2]^-$, **4**. The overall two-electron redox processes that generate these species are summarized in eqs 2 and 3.

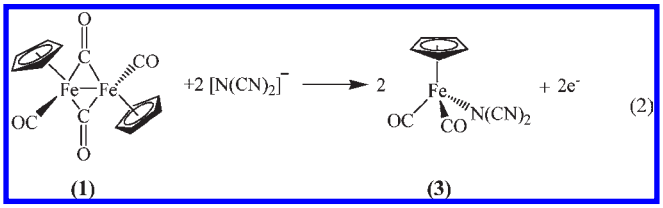


(2)

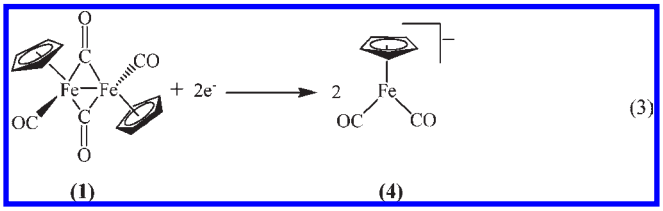


(3)

The products of each bulk process are electroactive, resulting in two coupled processes in the cyclic voltammogram, each of which leads to the regeneration of the starting compound, **1**. Specifically, the 18 electron product **3** is reduced by one-electron to the corresponding 19 electron species at 0.08 V versus $Cc^{+/0}$ (peak Ic), whereupon loss of the coordinated anion yields the 17 electron species, $CpFe(CO)_2$, **5**, which quickly dimerizes to **1**. Likewise, one-electron oxidation of the anion **4** to **5** at 0.0 V versus $Cc^{+/0}$ (peak IIa) also regenerates the parent dimer. These processes are summarized in eqs 4−6.

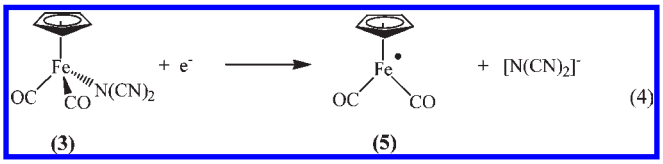


(4)

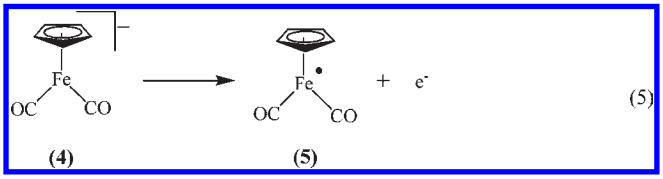


(5)

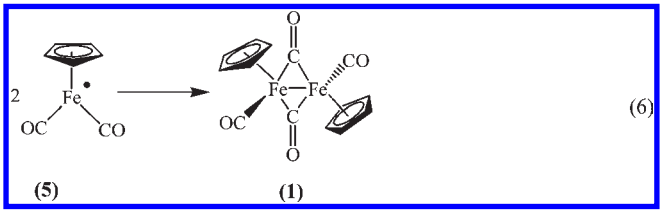


(6)

An additional feature accompanies the oxidation of **1** in [bmpyr][$N(CN)_2$]. A shoulder, labeled as peak IIIa in

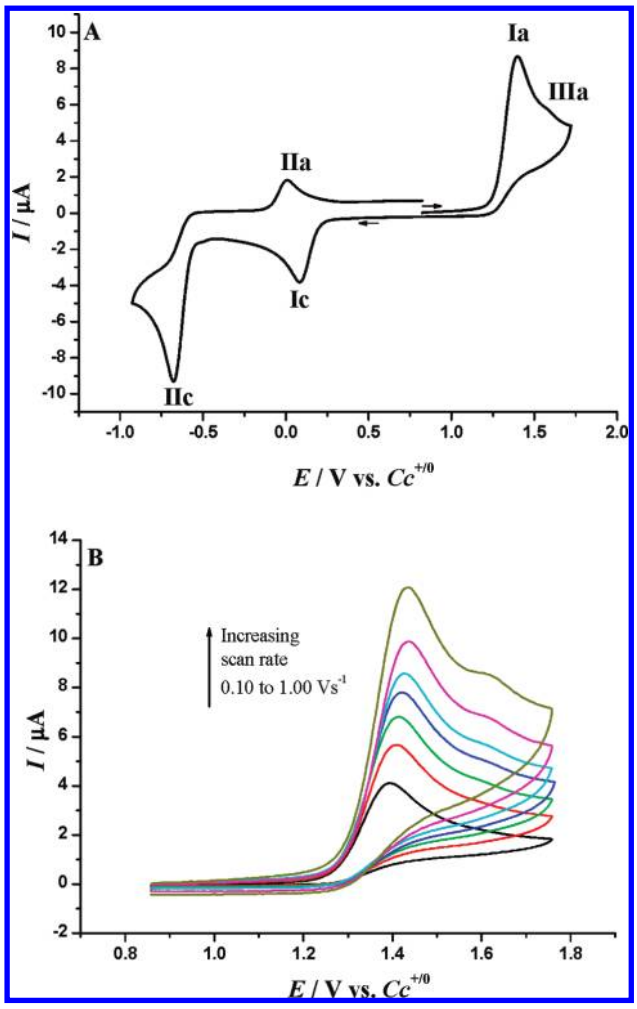


**Figure 1.** Cyclic voltammograms obtained for 7.00 mM **1** in [bmpyr][$N(CN)_2$] at a glassy carbon electrode ($d$ = 1 mm) (A) over a wide potential range with a scan rate of 0.50 V $s^{-1}$ and (B) over the potential region where the oxidation occurs at scan rates of 0.10, 0.20, 0.30, 0.40, 0.50, 0.70, and 1.00 V $s^{-1}$. $T = 21 \pm 1$ °C.

Figure 1, which becomes more pronounced at higher scan rates (Figure 1B), is seen at about 0.2 V more positive than process Ia. The net reaction described by eq 2 must therefore proceed via at least one intermediate. Insight into the nature of the intermediate and the overall mechanism can be gleaned from an earlier study[21] of the oxidation of **1** in $CH_2Cl_2$ ($Bu_4NPF_6$). During the course of a titration with $CH_3CN$ in the otherwise poorly coordinating medium, a peak 0.3 V more positive than the bulk oxidation process was observed in the presence of subequivalent levels of $CH_3CN$. This process was not present in the absence of $CH_3CN$ and was assigned to the oxidation of the $CH_3CN$ adduct of $\mathbf{1}^+$, $[CpFe(CO)_2]_2(CH_3CN)^+$. Since an analogous species is likely to be formed in [bmpyr][$N(CN)_2$], we assign the shoulder at 1.6 V versus $Cc^{+/0}$ to the oxidation of the dicyanamide adduct, $[CpFe(CO)_2]_2(N(CN)_2)$, **6**.

The direct observation of an intermediate in the oxidation of **1** in [bmpyr][$N(CN)_2$] supports a reaction scheme involving two competing ligand-induced ECE mechanisms, outlined below (Scheme 2). The initially formed $\mathbf{1}^+$ is rapidly attacked by dicyanamide to form **6** which, in turn, can follow one of two pathways. One possibility is

**Scheme 2.** Competing ECE Pathways for the Oxidation of **1** in [bmpyr][N(CN)$_2$]

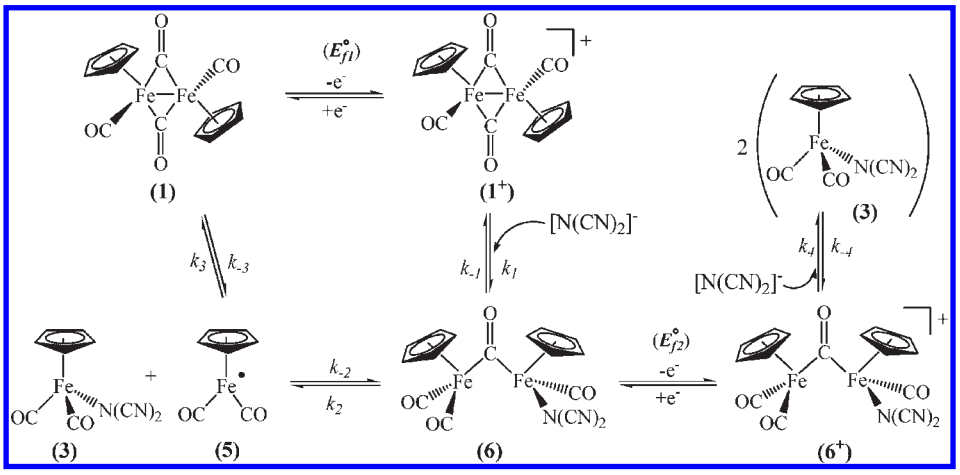

that **6** can be directly oxidized at the electrode, in process IIIa, which, after coordination to a second dicyanamide ion, yields 2 equiv of **3**. Alternatively, **6** can decompose unimolecularly to yield a single equivalent of **3** and the seventeen-electron monomer, **5**. The latter dimerizes to regenerate **1** which can be reoxidized at the electrode, resulting in current enhancement of the initial one-electron oxidation process. Interestingly, in the titration referred to above,[21] the oxidation peak assigned to [CpFe(CO)$_2$]$_2$-(CH$_3$CN)$^+$ becomes smaller at higher concentrations of added CH$_3$CN, indicating that this species is unstable toward further attack by the coordinating solvent; the peak is entirely absent when **1** is oxidized in CH$_3$CN (Bu$_4$NPF$_6$). The persistence of this voltammetric feature in neat [bmpyr][N(CN)$_2$] indicates that **6** is less susceptible toward further attack by the dicyanamide anion. Dicyanamide, being potentially a stronger nucleophile in this context, may stabilize **6** sufficiently that the rate constant governing the unimolecular decomposition step, $k_2$, becomes small enough that the [NTf$_2$]$^-$ adduct becomes long-lived enough to be readily observed via cyclic voltammetry at the moderate scan rates employed in these studies.

**3.2. Electrochemistry of 1 in Neutral [bmim][PF$_6$], [emim]-[NTf$_2$], and [bmpyr][NTf$_2$] ILs.** The electrochemistry of **1** also was examined in ILs whose anions nominally fall into the "neutral" category;[27] namely, [PF$_6$]$^-$, and [NTf$_2$]$^-$. Though we note that complexes of [PF$_6$]$^-$ and the [NTf$_2$]$^-$ are known,[15−17,22,30,31] the oxidation of **1** in these neutral ILs is considerably more reversible (Figures 2, 3 and Supporting Information, Figure S1) than that seen in the dicyanamide-based IL and occurs at potentials that are approximately 0.15 V more positive (Table 1). The potential shift is attributed to a combination of the effect of the coupled homogeneous reaction kinetics accompanying the electrode process and a difference in the stabilization of **1**$^+$ by the more strongly coordinating dicyanamide ion. As was the case in the basic IL, reduction of **1** is irreversible in these neutral ILs. However, the [bmpyr]$^+$-based ILs of neutral or basic anions give reduction peak potentials that are about 0.05 V more negative than those observed in the imidiazolium-based ILs. This may be due, in part, to preferential ion pairing of the reduction product, **4**, with the imidazolium cations, perhaps via $\pi-\pi$ interactions between the imidazolium ring and the cyclopentadienyl moiety of **4**.

Hexafluorophosphate has been widely employed as a supporting electrolyte anion in electrochemical work because of its very low Lewis basicity. However, it may not be completely innocent since there is evidence that it can coordinate to, or act as a nucleophile toward, highly electron-deficient species.[22,30,31] This aspect of its reactivity may be expected to be enhanced in IL media, since the [PF$_6$]$^-$ concentration in neat IL is roughly a factor of 50 greater than when it is employed as a supporting electrolyte in organic solvents, typically at a concentration of 0.10 M. Indeed, our results indicate that [PF$_6$]$^-$-based ILs have measurable reactivity toward electron-deficient species. For example, Figures 2B and 2C, which show the cyclic voltammetric response of the oxidation of **1** in [bmim][PF$_6$] obtained at scan rates between 0.05 and 1.00 V s$^{-1}$, reveal a decrease in peak current ratios at lower scan rates. We attribute this effect to a relatively slow attack by [PF$_6$]$^-$ on **1**$^+$ in a reaction analogous to that proposed for dicyanamide in Scheme 2. Such an interaction is consistent with the previously reported stabilization of [CpFe(CO)$_2$]$^+$ by [PF$_6$]$^-$.[21] We therefore assign the small coupled cathodic peak at 0.1 V in Figure 2A to the reduction of the [PF$_6$]$^-$ analogue of **3**.[32] While it is possible to attribute the slow reaction of **1**$^+$ to nucleophilic attack by adventititious water, we present evidence below that argues against this interpretation of the cyclic voltammetry data. Finally, the smaller diffusion coefficient of **1** in this IL (Table 1) is directly related to the higher viscosity (312 cP at 20 °C) and lower conductivity (1.40 mS cm$^{-1}$) of this IL compared to the others employed in this work.

The oxidation of **1** shows even greater chemical reversibility when performed in [NTf$_2$]$^-$-based ILs (Figure 3 and Supporting Information, Figure S1). The peak current ratios observed in these ILs are comparable to those reported in CH$_2$Cl$_2$ (Bu$_4$NPF$_6$)[21] and, in fact, approach those of ideal reversible electron transfers. For example,

(30) LeSuer, R. J.; Geiger, W. E. *Angew. Chem., Int. Ed.* **2000**, *39*, 248.
(31) Camire, N.; Nafady, A.; Geiger, W. E. *J. Am. Chem. Soc.* **2002**, *124*, 7260.

(32) Recognizing the potential for small amounts of water in [PF$_6$]$^-$−based ILs to react with the anion to produce F$^-$, and therefore the potential activity of F$^-$ as a ligand, we obtained the $^{19}$F NMR of this IL and found only resonances due to [PF$_6$]$^-$ in that spectrum.

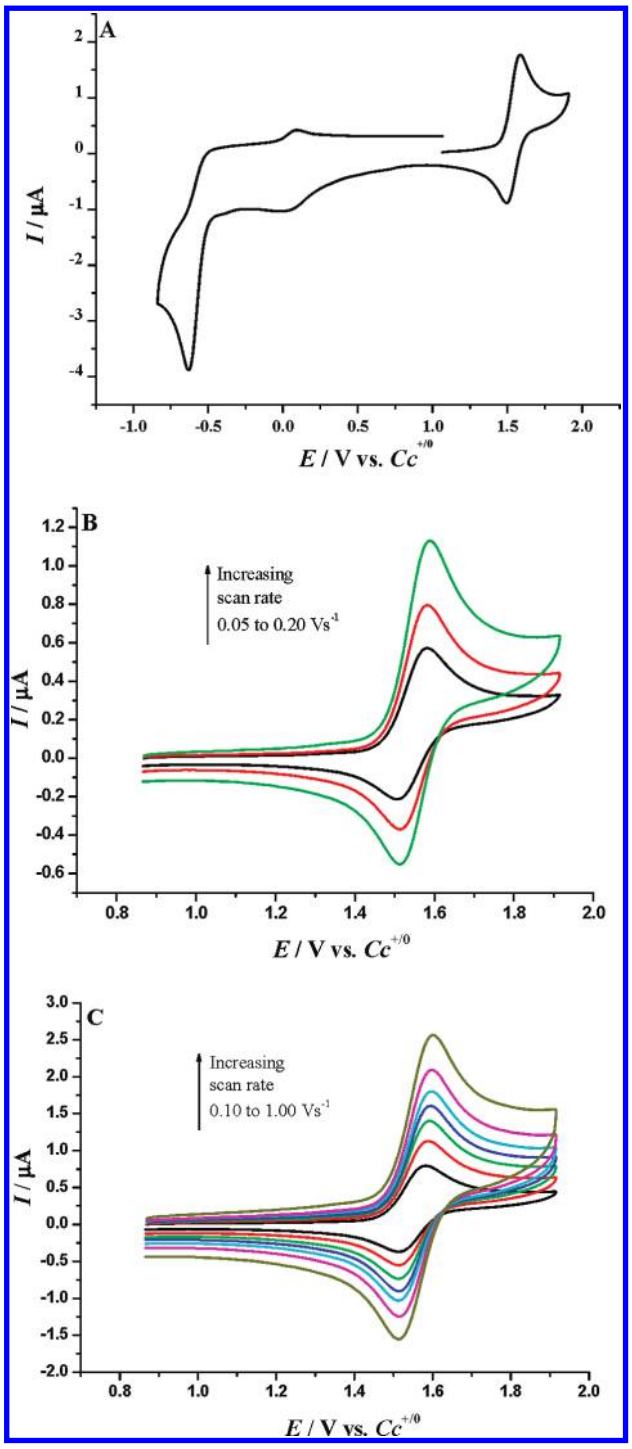


**Figure 2.** Cyclic voltammograms obtained for 7.00 mM **1** in [bmim][$PF_6$] at a glassy carbon electrode ($d$ = 1 mm) (A) over a wide potential range at a scan rate of 0.50 V $s^{-1}$ and (B) over the potential region where the oxidation occurs at scan rates of 0.05, 0.10, and 0.20 V $s^{-1}$, and (C) 0.10, 0.20, 0.30, 0.40, 0.50, 0.70, and 1.00 V $s^{-1}$. $T = 21 \pm 1$ °C.

the oxidative peak current of **1** in [bmpyr][$NTf_2$] varies linearly with the square root of scan rate over a range of 0.02 to 1.00 V $s^{-1}$ and with concentrations over the range $1.55-16.3 \times 10^{-4}$ mM (Supporting Information, Figure S1, C and D, respectively).

Despite the high level of reversibility of the $\mathbf{1}/\mathbf{1}^+$ couple in [$NTf_2$]$^-$-based ILs, there is still evidence of a slow homogeneous reaction coupled to the electron transfer.

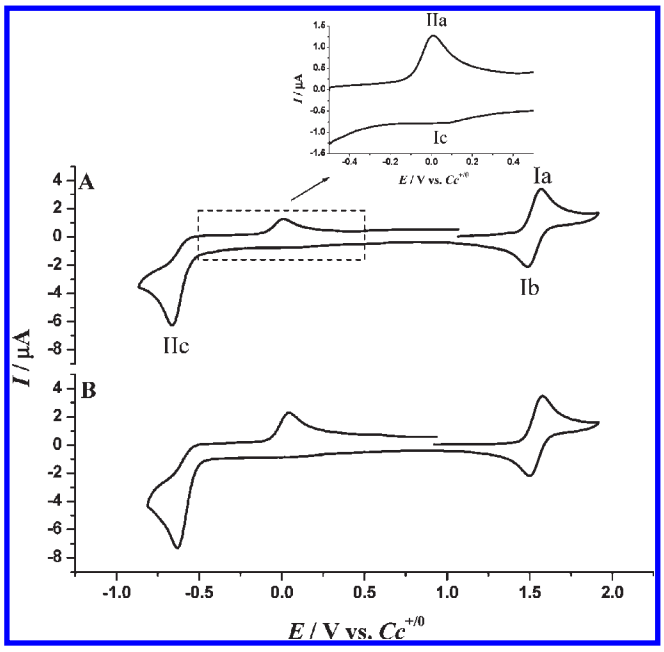


**Figure 3.** Cyclic voltammograms of 7.00 mM **1** in (A) [bmpyr][$NTf_2$] and (B) [emim][$NTf_2$] ILs over a wide potential range using a glassy carbon ($d$ = 1 mm) electrode. Scan rate = 0.50 V $s^{-1}$; $T = 21 \pm 1$ °C.

The expanded scale inset in Figure 3 reveals a small reduction current at about 0.0 V (peak Ic) coupled to the bulk oxidation; the current of this process increases relative to that of the bulk process at lower scan rates and is consistent with the formation of an [$NTf_2$]$^-$ adduct analogous to **6** in Scheme 2.

**3.3. Simulations of the Cyclic Voltammetry.** Although it is possible for [$NTf_2$]$^-$ to complex to metal carbonyls under some conditions (see, for example, the formation of $CpFe(CO)_2(NTf_2)$ from $CpFe(CO)_2CH_3$,[7] it exhibits remarkably slow kinetics as a nucleophile when employed as the anion in ILs.[33,34] To quantify the relative reactivity of the anions employed in this study, rate constants for the attack of the IL anion on $\mathbf{1}^+$ were estimated by fitting experimental voltammetric responses to digital simulations of the mechanism outlined in Scheme 2 (Figure 4). The simulations show excellent agreement with experimental observations when the rate constants, $k_1$, summarized in Table 1 are employed. Significantly, the rate constant for the reaction of [$NTf_2$]$^-$ (Figure 4A−F) toward $\mathbf{1}^+$ was found to be about one-third that for [$PF_6$]$^-$ (Figure 4 G−I), normally considered a relatively non-coordinating anion. Thus the reactivity toward $\mathbf{1}^+$ appears to be a usefully sensitive method of discriminating the relative nucleophilicity/basicity of IL anions. Moreover, simulations of the more complex chemistry in the dicyanamide-based IL also gave excellent agreement with the measured currents for the oxidation process IIIa over a wide range of scan rates when $k_1 = 450$ $s^{-1}$ and $k_2 = 80$ $s^{-1}$. The low $k_1$ values employed in the simulations of [$PF_6$]$^-$ and [$NTf_2$]$^-$-based ILs renders the simulation insensitive to the value of $k_2$ in these cases.

(33) Klingshirn, M. A.; Broker, G. A.; Holbrey, J. D.; Shaughnessy, K. H.; Rogers, R. D. *Chem. Commun.* **2002**, *13*, 1394.
(34) Wasserscheid, P.; Gordon, C. M.; Hilgers, C.; Muldoon, M. J.; Dunkin, I. R. *Chem. Commun.* **2001**, 1186.

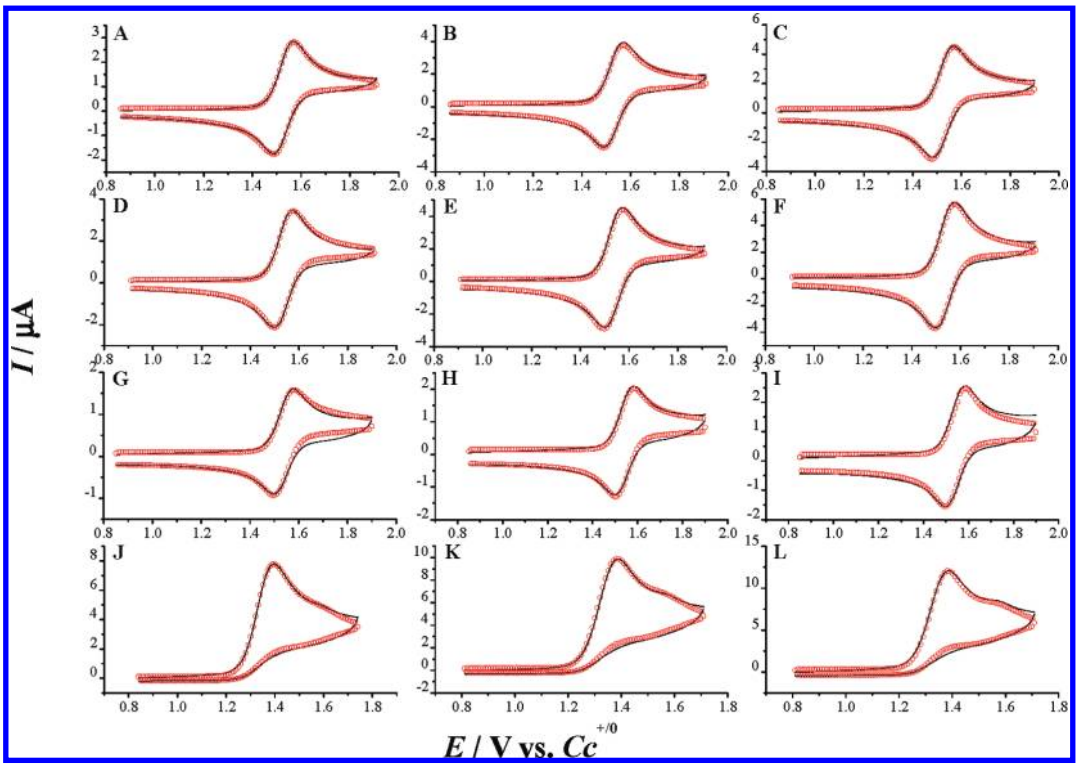


**Figure 4.** Comparison of experimental (solid lines) and simulated (open circles) cyclic voltammograms for the oxidation of **1** in (A−C) [bmpyr][$NTf_2$], (D−F) [emim][$NTf_2$], (G−I) [bmim][$PF_6$], and (J−L) [bmpyr][$N(CN)_2$]. The mechanism depicted in Scheme 2 was used for simulations. Scan rates = (A, D, G, J) 0.40 V $s^{-1}$; (B, E, H, K) 0.70 V $s^{-1}$; and (C, F, I, L) 1.00 V $s^{-1}$. For all simulations: $T$ = 294 K, electrode area = 0.007237 $cm^2$, charge-transfer coefficient ($\alpha$) = 0.5, heterogeneous standard rate constant ($k_s$) = 1.0 × $10^4$ cm $s^{-1}$, equilibrium constant ($K_{eq}$) for all reactions = 1 × $10^4$, $c_1$ = 7.00 mM. For A−C: reversible potential, $E_{f1}°$ = 1.53 V vs $Cc^{+/0}$, $k_1$ = 0.58 $s^{-1}$, $C_{dl}$ = 0.30 $\mu$F, $D$ (for all species) = 1.05 × $10^{-7}$ $cm^2$ $s^{-1}$. For D−F: $E_{f1}°$ = 1.54 V vs $Cc^{+/0}$, $k_1$ = 0.48 $s^{-1}$, double-layer capacitance ($C_{dl}$) = 0.20 $\mu$F, $D$ (for all species) = 1.45 × $10^{-7}$ $cm^2$ $s^{-1}$. For G−I: $E_{f1}°$ = 1.54 V vs $Cc^{+/0}$, $k_1$ = 1.50 $s^{-1}$, $C_{dl}$ = 0.20 $\mu$F, $D$ (for all species) = 0.25 × $10^{-7}$ $cm^2$ $s^{-1}$. $k_2$, $k_3$, and $k_4$ = included in simulations A−I, and have no significant effect. For J−L: $E_{f1}°$ = 1.35 V and $E_{f2}°$ = 1.59 V vs $Cc^{+/0}$, $k_1$ = 450 $s^{-1}$, $k_2$ = 80 $s^{-1}$, $k_3$ = 1.0 × $10^7$ $s^{-1}$, $k_4$ = 1.0 × $10^4$ $s^{-1}$, $C_{dl}$ = 0.30 $\mu$F, $D$ (for all species) = 3.60 × $10^{-7}$ $cm^2$ $s^{-1}$.

Also, the observed numerical values of $k_s$, $\alpha$, and $K_{eq}$ are not significant but are used to achieve reversibility or other features, as appropriate.

**3.4. Effect of Water.** As noted above, $\mathbf{1}^+$ is susceptible to attack by water, a virtually ubiquitous impurity in ILs. In neutral ILs water can act as a relatively strong nucleophile. The water content of the ILs employed in this work was monitored by Karl Fisher titration and maintained at a constant value of 80 ± 10 ppm. To support our contention that the relatively slow chemical reactions of $\mathbf{1}^+$ observed in neutral ILs is primarily due to the IL anion and not to adventitious water, we examined the cyclic voltammetry of **1** in [emim][$NTf_2$] after the deliberate introduction of additional water. Under these conditions, a new irreversible reduction process coupled to the oxidation of **1** appears at ~0.63 V versus $Cc^{+/0}$ well positive of the coupled process observed in the neutral ILs without added water; this peak is indicated with the asterisk in Figure 5. Based in Scheme 2, attack by water on $\mathbf{1}^+$ is expected to result in formation of $[CpFe(CO)_2(H_2O)]^+$ and, accordingly, this new peak is assigned to its one-electron reduction, a process analogous to that described by eq 4.

**3.5. Electrochemistry of 1 and 1* in $CH_2Cl_2$ (0.5 M [bmpyr][$NTf_2$]).** Recently, there has been considerable interest in very weakly coordinating media for electrochemical work.[6] The very low nucleophilicity exhibited by $[NTf_2]^-$ suggests that [emim][$NTf_2$] and [bmpyr][$NTf_2$] may serve as readily available non-coordinating electrolytes in molecular solvents. To explore this possibility, we

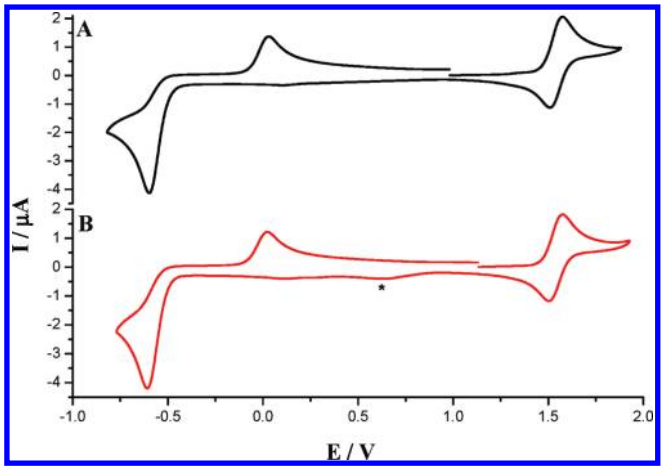


**Figure 5.** Cyclic voltammograms at a glassy carbon electrode ($d$ = 1 mm) in [emim][$NTf_2$] for (A) 7.30 mM of **1** and 80 ± 10 ppm of water and (B) 7.00 mM of **1** and 160 ± 10 ppm of water. Scan rate = 0.10 V $s^{-1}$, $T$ = 21 ± 1 °C. Water concentrations were determined by Karl Fischer titration. The peak marked with the asterisk is assigned to the reduction of the water adduct, $CpFe(CO)_2(H_2O)]^+$.

examined the behavior of [bmpyr][$NTf_2$] as a supporting electrolyte in $CH_2Cl_2$. Oxidation of 1 mM **1** in $CH_2Cl_2$ (0.50 M [bmpyr][$NTf_2$]) showed close to ideal cyclic voltammetric behavior, with the midpoint potential, $E_m$, ($\approx E°_f$) of 1.53 V versus $Cc^{+/0}$ and peak current ratios close to unity, increasing from 0.95 to 0.99 when the scan rate was increased from 0.1 to 1.0 V $s^{-1}$. The peak-to-peak

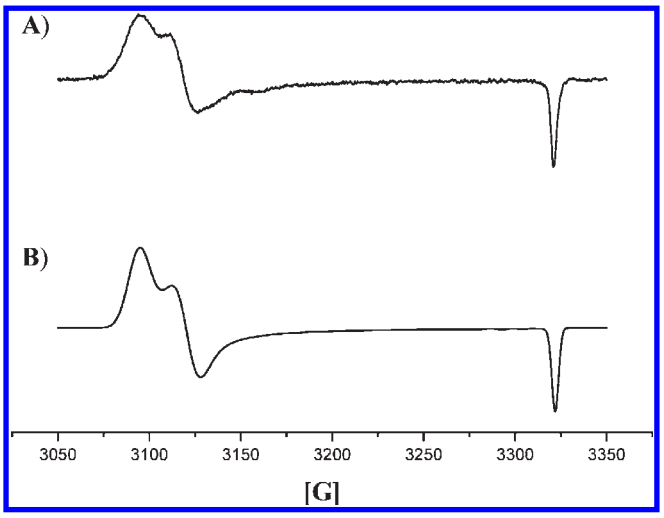


**Figure 6.** Experimental (A) and simulated (B) EPR spectra for electrolytically generated $\mathbf{1}^+$ in $CH_2Cl_2$ (0.50 M [bmpyr][$NTf_2$]). Experimental conditions: $T$ = 77 K; microwave frequency = 9.299 GHz; microwave power = 0.525 mW; 100 kHz modulation amplitude = 1.0 G; field scan = 300 G/83.9 s; receiver gain = $2.0 \times 10^5$; time constant = 81.9 ms. Simulation: Gaussian line shape (cutoff 10); g-values and linewidths as shown in Table 2.

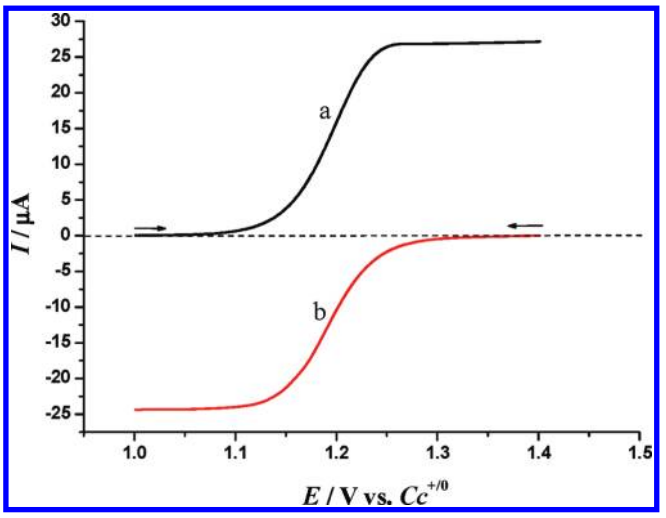


**Figure 7.** Rotating disk electrode voltammograms obtained at a glassy carbon electrode ($d$ = 3 mm) (a) before and (b) after exhaustive bulk oxidative electrolysis of a 0.96 mM **1*** in $CH_2Cl_2$ (0.5 M [bmpyr][$NTf_2$]) at a potential of 1.40 V vs $Cc^{+/0}$ . Rotation rate = 500 rpm; scan rate = 0.02 V $s^{-1}$.

**Table 2.** g-Values and Linewidths Obtained from Simulation of the EPR Spectra of $\mathbf{1}^+$ and $\mathbf{1}^{*+}$ Produced by Electrolytic Oxidation of $\mathbf{1}^+$ and **1*** in $CH_2Cl_2$ (0.5 M [bmpyr][$NTf_2$])[a]

| complex | parameter | temperature (K) | $X$ | $Y$ | $Z$ |
|---|---|---|---|---|---|
| $\mathbf{1}^+$ | g-value | 77 | 2.1475 | 2.1300 | 2.0005 |
| | | 160 | 2.1490 | 2.1290 | 2.0020 |
| | linewidth ($\times 10^{-4}$ $cm^{-1}$) | 77 | 7.00 | 7.00 | 2.00 |
| | | 160 | 15.0 | 7.50 | 5.00 |
| $\mathbf{1}^{*+}$ | g-value | 77 | 2.1330 | 2.1060 | 1.9985 |
| | | 175 | 2.1240 | 2.1033 | 2.0068 |
| | linewidth ($\times 10^{-4}$ $cm^{-1}$) | 77 | 10.0 | 5.50 | 3.00 |
| | | 175 | 8.00 | 8.00 | 8.00 |

[a] The lineshapes used were Gaussian at 77 K and Lorentzian at 160 K ($\mathbf{1}^+$) and 175 K ($\mathbf{1}^{*+}$). Uncertainties in the g-values were estimated as ±0.0003 at 77 K and ±0.0005 at 160 or 175 K. Uncertainties in the linewidths were estimated as $\pm 0.5 \times 10^{-4}$ $cm^{-1}$.

potential separation ($\Delta E_p$) was 69 mV at 0.1 V $s^{-1}$. BE of 1.0 mM **1** at a GC working electrode at 1.8 V versus $Cc^{+/0}$ passed 1.0 ± 0.1 electrons per starting dimer and yielded purple solutions that are characteristic of $\mathbf{1}^+$.[21] The EPR spectrum obtained at 77 K of $\mathbf{1}^+$ generated by the bulk electrolyses described above is shown in Figure 6A and is consistent with the presence of only a single species; there was no indication of hyperfine structure. The spectrum was simulated using the orthorhombic g-values and linewidths listed in Table 2 and is shown in Figure 6B. Although the g-matrix and molecular axes cannot be correlated without a single crystal EPR study, it is reasonable to propose that the direction of $g_z$ approximates the Fe−Fe bond direction and that the directions of $g_x$ and $g_y$ are in a plane perpendicular to this, very approximately in the plane of the Cp rings.

EPR spectra were also obtained over the temperature range from 77 to 160 K. As the temperature increases, the relative intensities of the peaks associated with $g_x$ and $g_y$ shift and the shape of the resonance associated with $g_z$ took on a more Lorentzian appearance. These changes would appear to be due to the onset of motional and/or vibrational effects as the solvent approaches its melting point where the constraints on the motion of the Cp rings imposed by the frozen solvent molecules are reduced.

In contrast to the above results, bulk electrolyses of **1** in neat [bmpyr][$NTf_2$] yield solutions that are EPR silent. This difference is attributed to the much longer time (4 h vs 5 min) required for exhaustive oxidation in the neat IL, a result of the much higher viscosity (0.39 cP for $CH_2Cl_2$ at 30 °C vs 85 cP for [bmpyr][$NTf_2$] at 25 °C), and therefore lower mass transport rate, compared to conventional solvent systems. Consequently, $\mathbf{1}^+$, while stable on the cyclic voltammetry time-scale, is susceptible to attack by the anion or adventitious water on the much longer BE time scale required in neat [bmpyr][$NTf_2$].

The cyclic voltammetry of **1***, the permethylated analogue of **1**, also exhibits a nearly ideally reversible one-electron process in $CH_2Cl_2$ (0.50 M [bmpyr][$NTf_2$]) at a glassy carbon electrode (Supporting Information, Figure S2; $E_m$ = 1.20 V vs $Cc^{+/0}$; $I_p^{red}/I_p^{ox}$ = 0.95; $D = 7.35 \times 10^{-6}$ $cm^2$ $s^{-1}$). The lower reversible potential of **1*** ($E_m$ is 0.33 V less positive than for **1**) is due to the enhanced electron-donating ability of the Cp* ligand relative to Cp. Bulk oxidation of **1*** in $CH_2Cl_2$/0.50 M [bmpyr][$NTf_2$] yielded an $n$ value of 0.97 ± 0.02 electrons per molecule and exhibited an exponential current decay as expected for an E mechanism. RDE voltammograms obtained before and after BE (Figure 7) changed from a reversible one-electron oxidation (curve a) to a one-electron reduction process (curve b) and indicate that almost quantitative conversion of **1*** to $\mathbf{1}^{*+}$ occurs on this time scale (tens of minutes). Bulk reduction of $\mathbf{1}^{*+}$ that had been previously generated by oxidative BE was similarly well-behaved; coulometric data indicated an $n$ value of 0.93 ± 0.02.

$\mathbf{1}^{*+}$ was also characterized by EPR spectroscopy (Figure 8A). The spectrum at 77 K initially appeared to be interpretable in terms of a system with orthorhombic g-values and linewidths. However, the peak associated with $g_x$ (the largest g-value) could not be readily simulated,

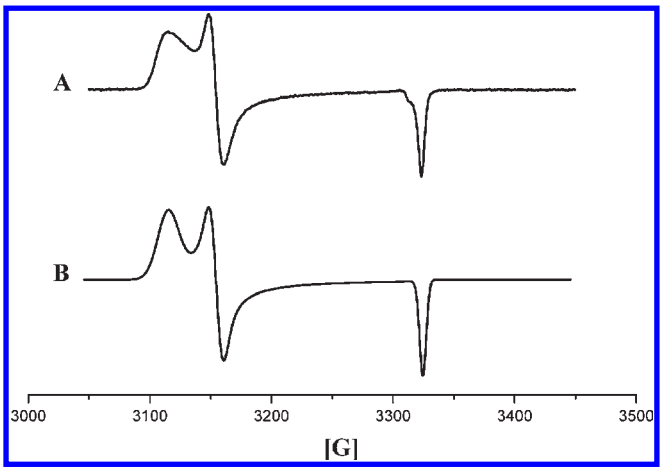


**Figure 8.** Experimental (A) and simulated (B) EPR spectra for electrolytically generated $\mathbf{1}^{*+}$ in $CH_2Cl_2$ (0.50 M [bmpyr][$NTf_2$]). Experimental conditions: $T$ = 77 K; microwave frequency = 9.310 GHz; microwave power = 0.525 mW; 100 kHz modulation amplitude = 1.00 G; field scan = 400 G/83.9 s; receiver gain = $1.0 \times 10^5$; time constant = 41 ms. Simulation: Gaussian line shape (cutoff 10); g-values and linewidths as shown in Table 2.

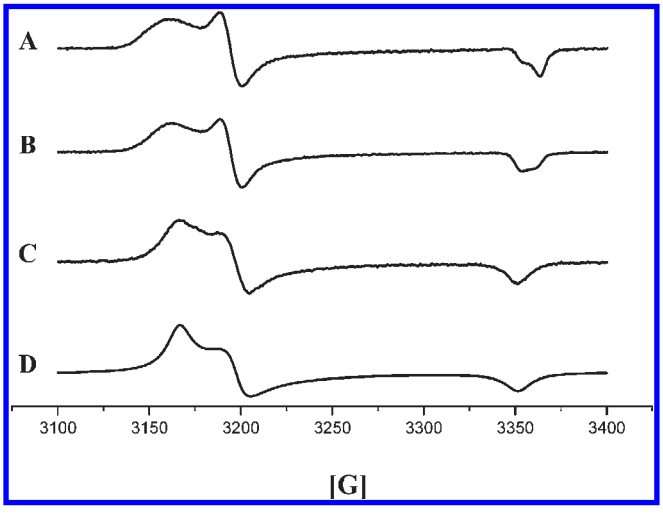


**Figure 9.** Experimental (A, B, and C) and simulated (D) EPR spectra for electrolytically generated $\mathbf{1}^{*+}$ in $CH_2Cl_2$ (0.50 M [bmpyr][$NTf_2$]). Experimental conditions: temperatures = (A) 110 K; (B) 135 K; (C) 175 K; microwave frequency = 9.423 GHz; microwave power = 0.525 mW; 100 kHz modulation amplitude = 1.00 G; field scan = 300 G/41.9 s; receiver gain = $1.0 \times 10^5$; time constant = 41 ms. (D) Simulation of 175 K spectrum: Lorentzian line shape (cutoff 10); g-values and linewidths as shown in Table 2.

and there appeared to be a resonance at a slightly lower field than the resonance due to $g_z$, the smallest g-value (Figure 8B). These observations imply the presence of a second, minor, species. As the temperature was raised (Figure 9), this second species increased in intensity while the intensity of the first decreased, until at 175 K only the second species was present. The appearance of the peak due to $g_z$ at 175 K resembled that observed for the $g_z$ peak at a similar temperature for the non-methylated species, the appearance of which was attributed to motional effects. Double integrations of the first derivative spectra (i.e., the area under the absorption curve) as a function of temperature showed that the number of paramagnetic species remained unchanged over the temperature range of 110 to 175 K.

The EPR spectra differ slightly to those reported previously[21] most probably because of the use of a different solvent and the accessibility of a greater range of temperatures in the present study. In particular, the addition of electrolyte appears to result in the formation of better glasses on freezing and hence to better resolved spectra. The g-values of both samples are consistent with the formation of radical species where the unpaired electron is delocalized between the two Fe ions via a $\sigma$ bonding interaction. Moreover, these results are not consistent with other possible iron species: $Fe^{3+}$ and $Fe^{1+}$ high spin and low spin forms are expected to give quite different g-values, and the low spin $Fe^{3+}$, as well as both possible spin states of $Fe^{1+}$, usually require low temperatures (< 100 K) for their observation.[35] However, the inability to observe hyperfine structure precludes the possibility of estimating Fe−Fe bonding,[36] contrasting the case of the $Cp(Co)_2$ dimer in which the involvement of 2 equiv of Co ions is shown by the 15 line hyperfine structure.[37]

There is a small but significant difference in the g-values of $\mathbf{1}^+$ and $\mathbf{1}^{*+}$ (major species) at 77 K, that is likely due to the inductive effect of the methyl groups of Cp*.[38] Moreover, the existence of two similar spectra for $\mathbf{1}^{*+}$ from 77 K to about 160 K is interesting and worthy of comment. Infrared data indicate $\mathbf{1}^{*+}$ assumes only the *trans* geometry,[21] whereas $\mathbf{1}^+$ can exist as the *cis* or *trans* form. That only one spectrum is observed at all temperatures in the range from 77 to 160 K for $\mathbf{1}^+$ would appear to exclude the possibility that the two spectra of $\mathbf{1}^{*+}$ are due to *cis* and *trans* isomers. Rather, we speculate that they are due to the steric demands of the Cp* ligand and the expected barrier to rotation about its $C_5$ axis at very low temperature. Specifically, the Cp* ligands may be frozen into multiple orientations at 77 K, whereas the smaller Cp ligand may continue to rotate under the same conditions. Thus, the spectrum of $\mathbf{1}^+$ is the average of the spectra resulting from all possible orientations of the Cp rings but that for $\mathbf{1}^{*+}$ reflects the contributions of two structural forms that do not interconvert. As the temperature increases, these rings can rotate more rapidly, and the resultant spectrum is the average of all possible orientations. This average is the spectrum observed at the higher temperatures. This model explains why the overall number of Fe−Fe systems remains constant even though the low temperature spectrum (predominant at 77 K) is gradually replaced by that observed at 175 K.

## 4. Conclusion

The present study demonstrates the large IL medium effect on the chemical reversibility for the oxidation of **1** and hence illustrates the wide range of electrochemical environments

(35) Nafady, A.; Costa, P. J.; Calhorda, M. J.; Geiger, W. E. *J. Am. Chem. Soc.* **2006**, *128*, 16587.

(36) Hyperfine resonances due to $^{57}Fe$ are expected to be of very low intensity because of the low abundance of this isotope ($I$ = 1/2, 2.15%) and the hyperfine splitting is expected to be small (ca. 1/10th of that of $^{59}Co$) and most likely submerged under the resonances due to the predominant nonmagnetic $^{56}Fe$ isotope.

(37) Pilbrow, J. R. In *Transition Ion Electron Paramagnetic Resonance*; Clarendon Press: Oxford, 1990; p 138.

(38) Zanello, P. *Inorganic Electrochemistry: Theory, Practice and Application*; The Royal Society of Chemistry: Cambridge, U.K., 2003.

available with ILs. With over 200 different ILs currently available commercially and many others readily synthesized in a research laboratory, it should be possible, by judicious choice of the specific cations and anions used, to tune the properties of IL based electrochemical media for a host of applications, including those requiring exceptionally non-coordinating conditions.

The differences in the voltammetric behavior of **1** reveal several interesting aspects of the IL media. Most notably, the chemical reversibility of the $\mathbf{1}^{0/+}$ couple is highly dependent on the basicity of the IL anion. When $[NTf_2]^-$ is the anion, the couple showed acceptable chemical reversibility, even at low scan rates, whereas when $[N(CN)_2]^-$ was employed, the oxidation process was clearly irreversible, resembling that obtained in acetonitrile. Moreover, our results indicate that when used as supporting electrolytes in non-polar molecular solvents, $[NTf_2]^-$-based ILs have the potential to be less nucleophilic than the very commonly employed $[PF_6]^-$ salts.

**Acknowledgment.** We are grateful to the Australian Research Council-Orica Linkage Grant LP0668123 and Monash University for provision of facilities and financial support of this project.

**Supporting Information Available:** Cyclic voltammograms over the potential region where oxidation occurs and their dependence on scan rate and concentration for 7.0 mM **1** in [bmpyr][$NTf_2$] and [emim][$NTf_2$], cyclic voltammograms obtained for oxidation of 0.96 mM **1*** in $CH_2Cl_2$ (0.50 M [bmpyr][$NTf_2$]) at different scan rates. This material is available free of charge via the Internet at http://pubs.acs.org.